Electrochemical synthesis of fluorescence-enhanced carbon dots with multicolor emission via surface nitrogen and sulfur modulation for information encryption applications

Qingling Zhao[a], Xiaotong Wang[a], Qinghong Song[b], Zehao Zang[a], Chunyan Fan[a], Lanlan Li[a], Xiaofei Yu[a], Xiaojing Yang[a], Zunming Lu[a], and Xinghua Zhang[a,*]

[a]School of Materials Science and Engineering, Hebei University of Technology, Tianjin 300130, China,

[b]Tianjin Peoples Hospital, Tianjin 300122, China

[*]Corresponding author, Email: zhangxinghua@hebut.edu.cn

Supporting information

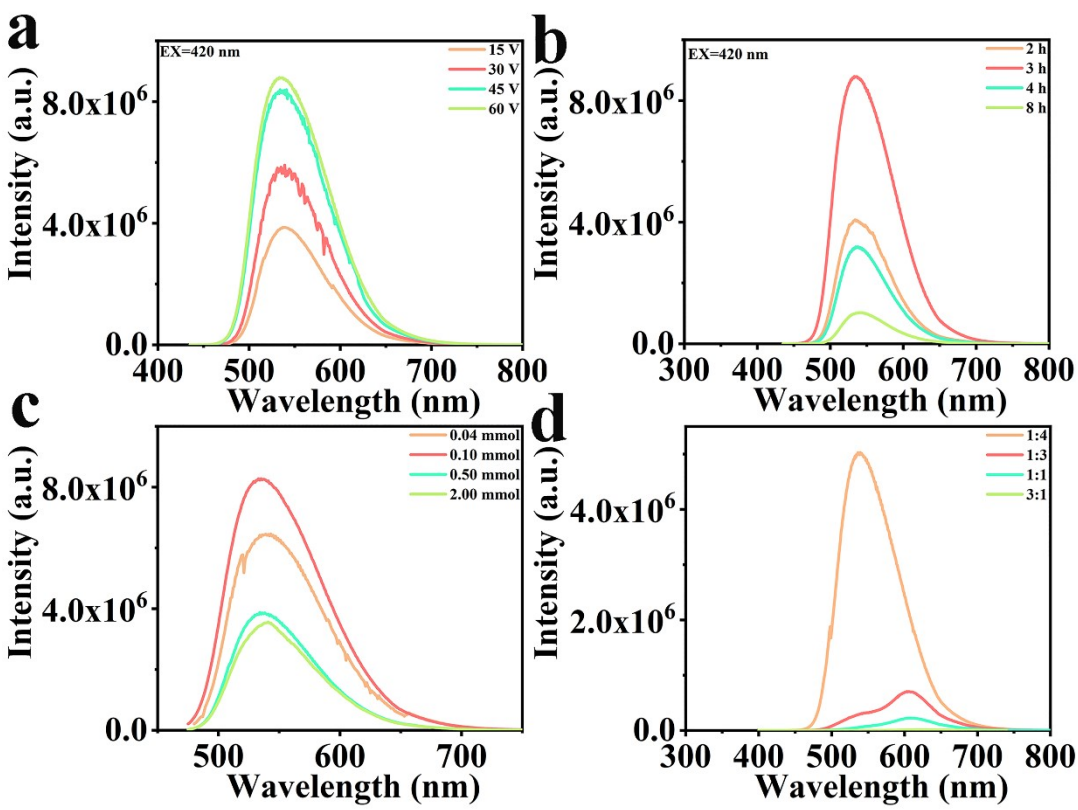

Fig. S1. Emission spectra of N-GCDs prepared with (a) different applied voltages, (b) various reaction times and (c) different contents of o-phenylenediamine under excitation of 460 nm, (d) emission spectra of N-RCDs synthesized with different ratios of p-phenylenediamine and o-phenylenediamine from 1:4 to 3:1 under excitation at 460 nm.

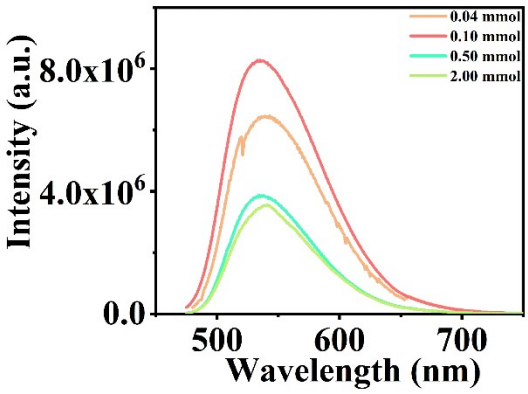

Fig. S2. Emission spectra of N,S-GCDs synthesized with different contents of thioacetamide under excitation at 420 nm.

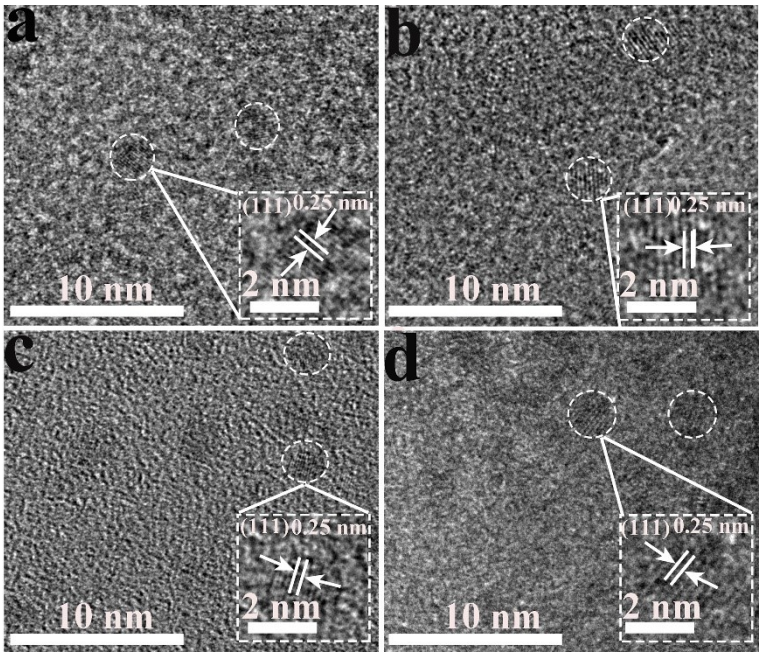

Fig. S3. HRTEM images of (a) OCDs, (b) N,S-BCDs, (c) N,S-GCDs, and (d) N,S-RCDs.

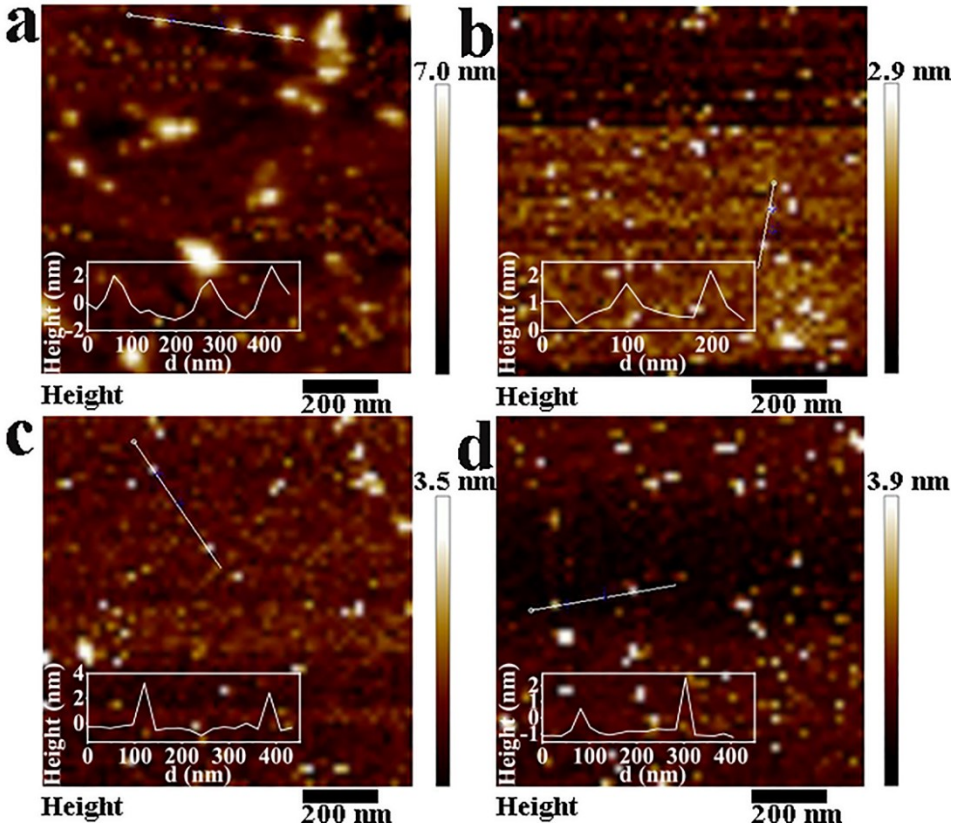

Fig. S4. AFM images of (a) OCDs, (b) N,S-BCDs, (c) N,S-GCDs, and (d) N,S-RCDs.

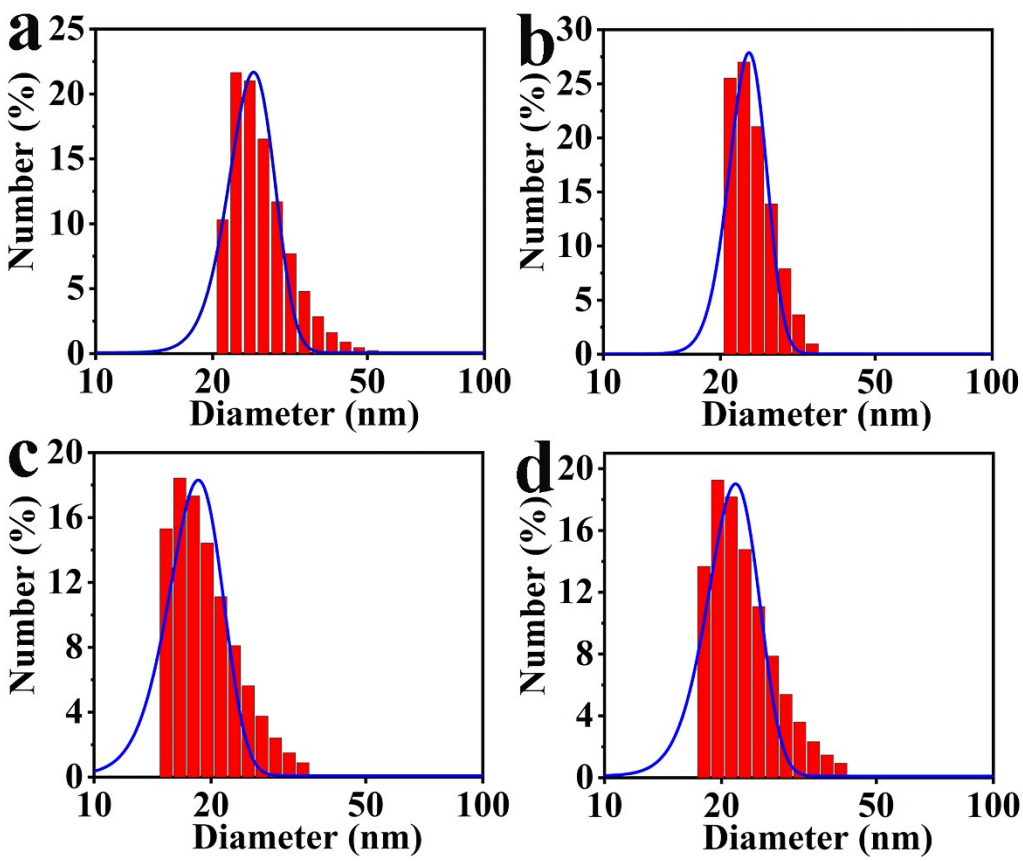

Fig. S5. Hydrodynamic diameter of(a) OCDs, (b) N,S-BCDs, (c) N,S-GCDs, and (d) N,S-RCDs in an aqueous medium from DLS measurement.

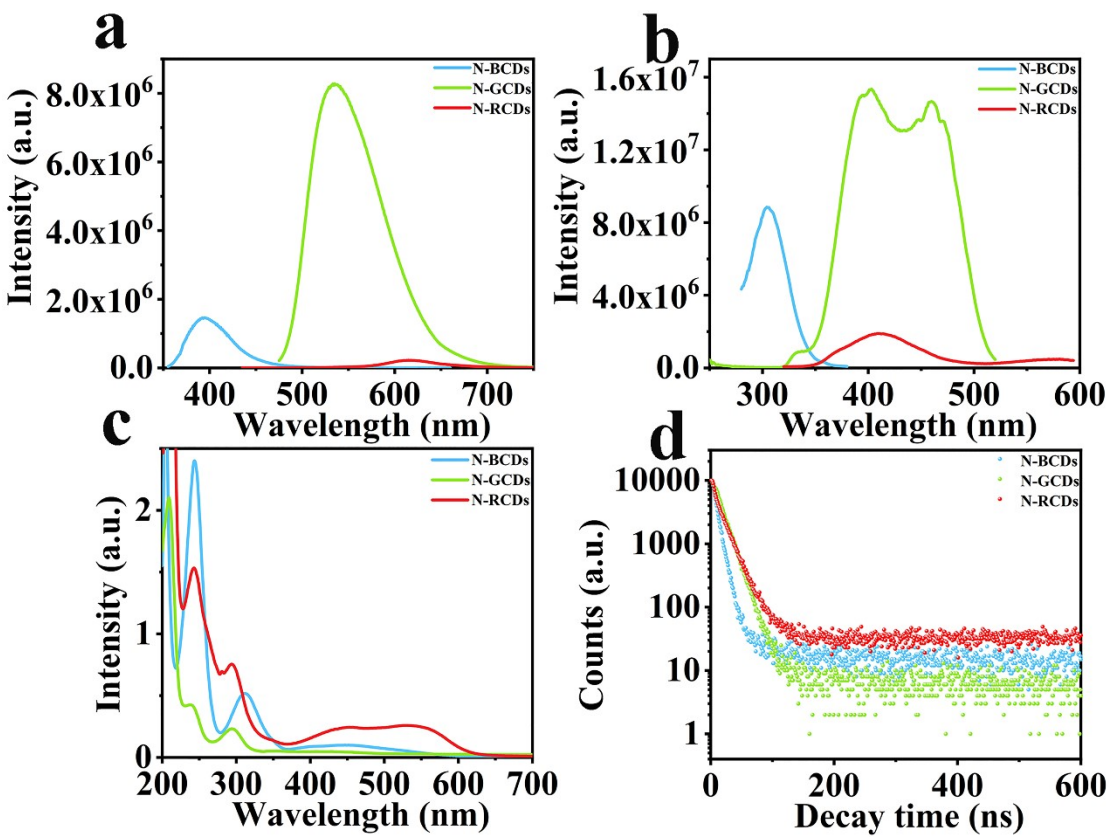

Fig. S6. (a) The optimal emission spectra of N-BCDs, N-GCDs and N-RCDs under excitation at 340 nm, 420 nm and 380 nm, respectively. (b) Excitation spectra with emission at 400 nm, 541 nm and 614 nm, respectively. (c) UV−vis absorption spectra and (d) fluorescence decay curves of N-BCDs, N-GCDs and N-RCDs.

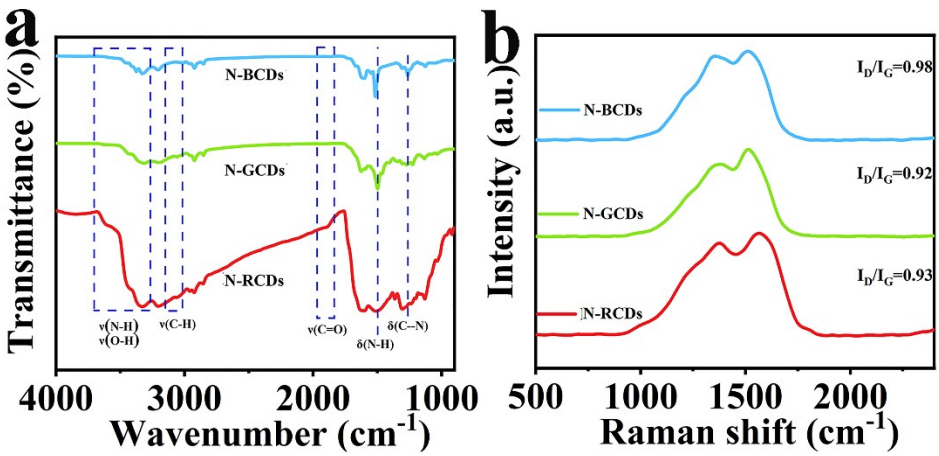

Fig. S7. (a) FTIR spectra and (b) Raman spectra of N-BCDs, N-GCDs and N-RCDs.

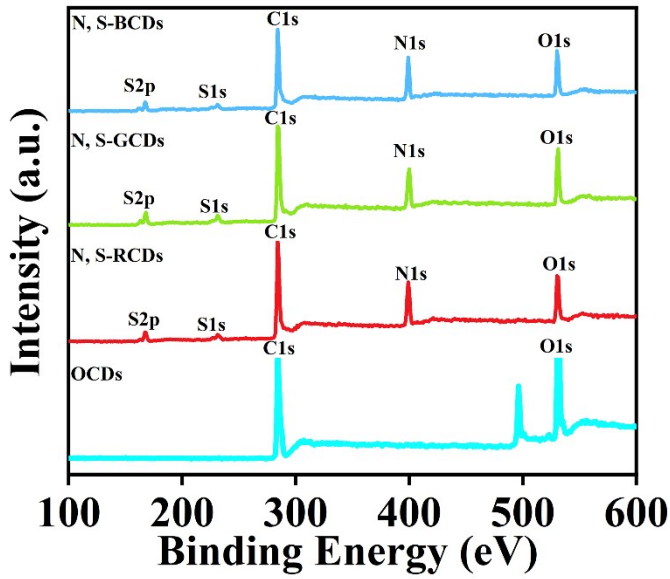

Fig. S8. XPS spectra of OCDs, N,S-BCDs, N,S-GCDs, and N,S-RCDs.

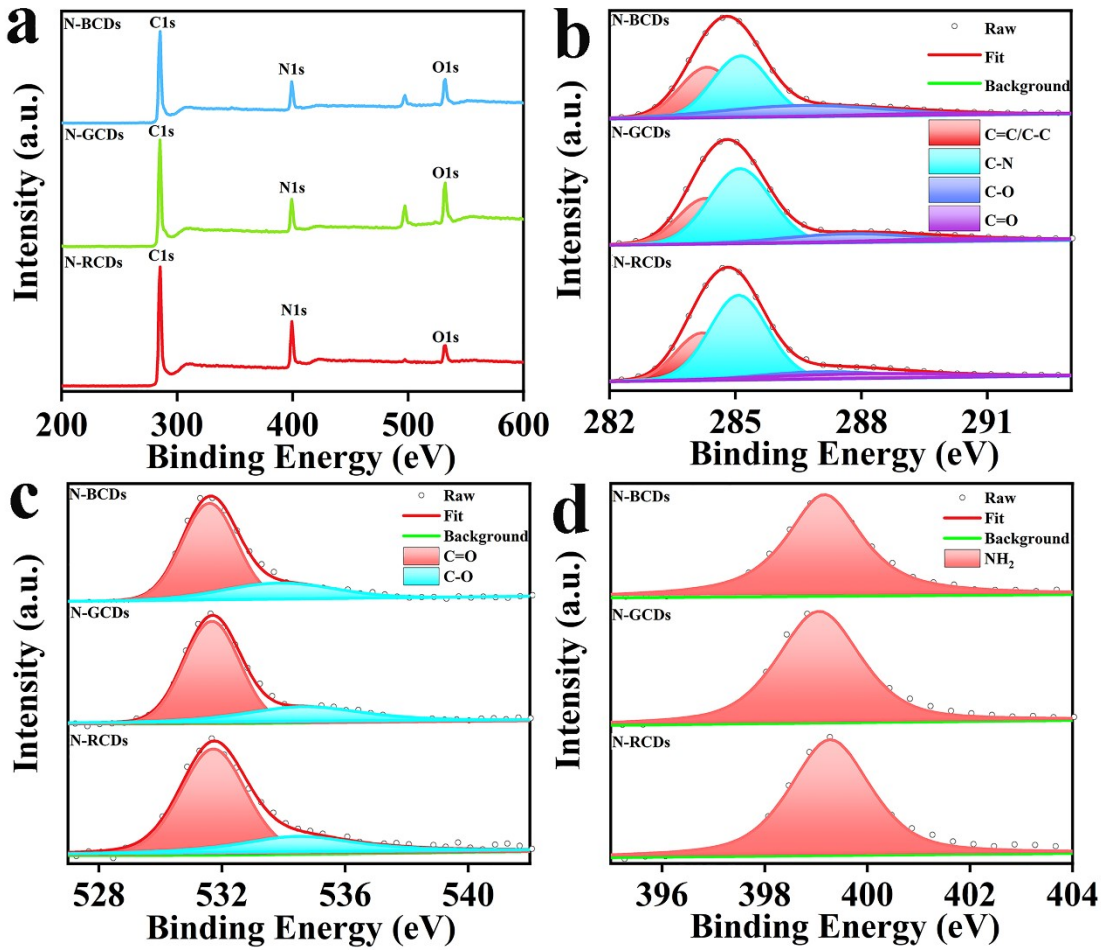

Fig. S9. (a) XPS survey scan and high-resolution XPS spectra of (b) C1s, (c) O1s, and (d) N1s for N-BCDs, N-GCDs and N-RCDs.

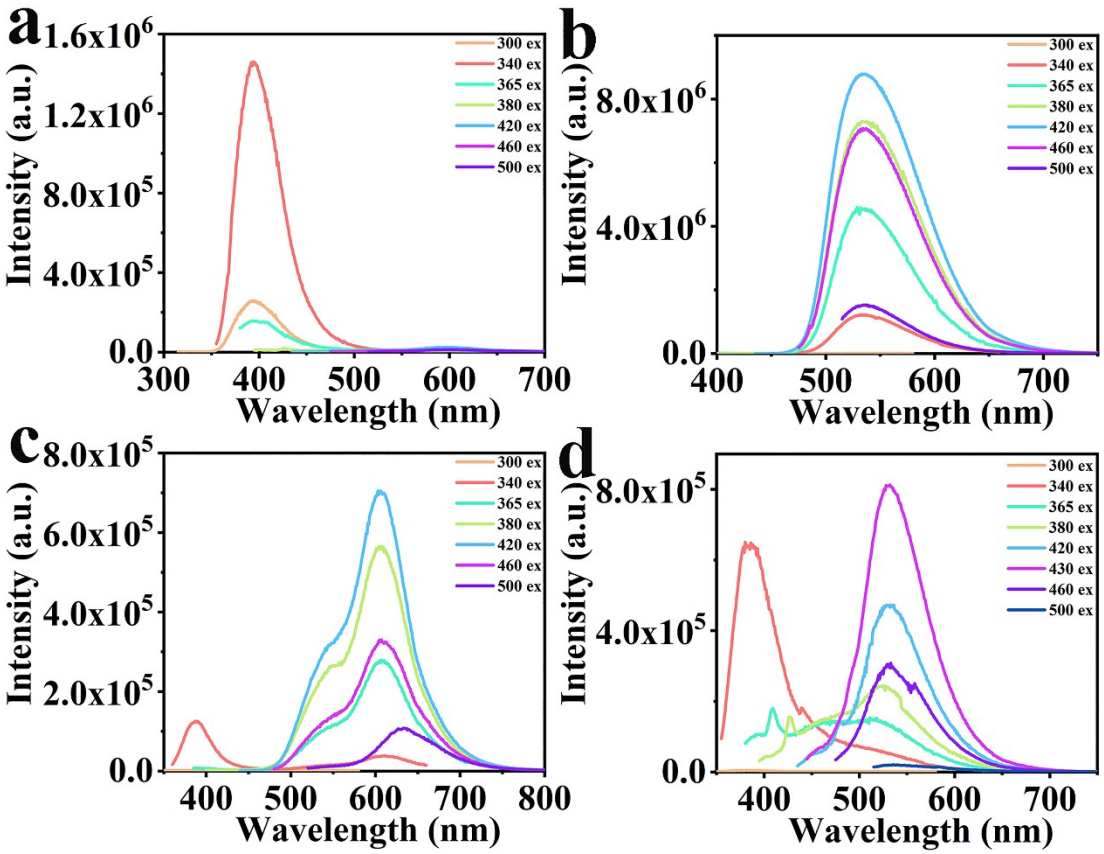

Fig. S10. Emission spectra of (a) N-BCDs, (b) N-GCDs, (c) N-RCDs and (d) S-CDs under different excitation wavelengths (300 -500 nm).

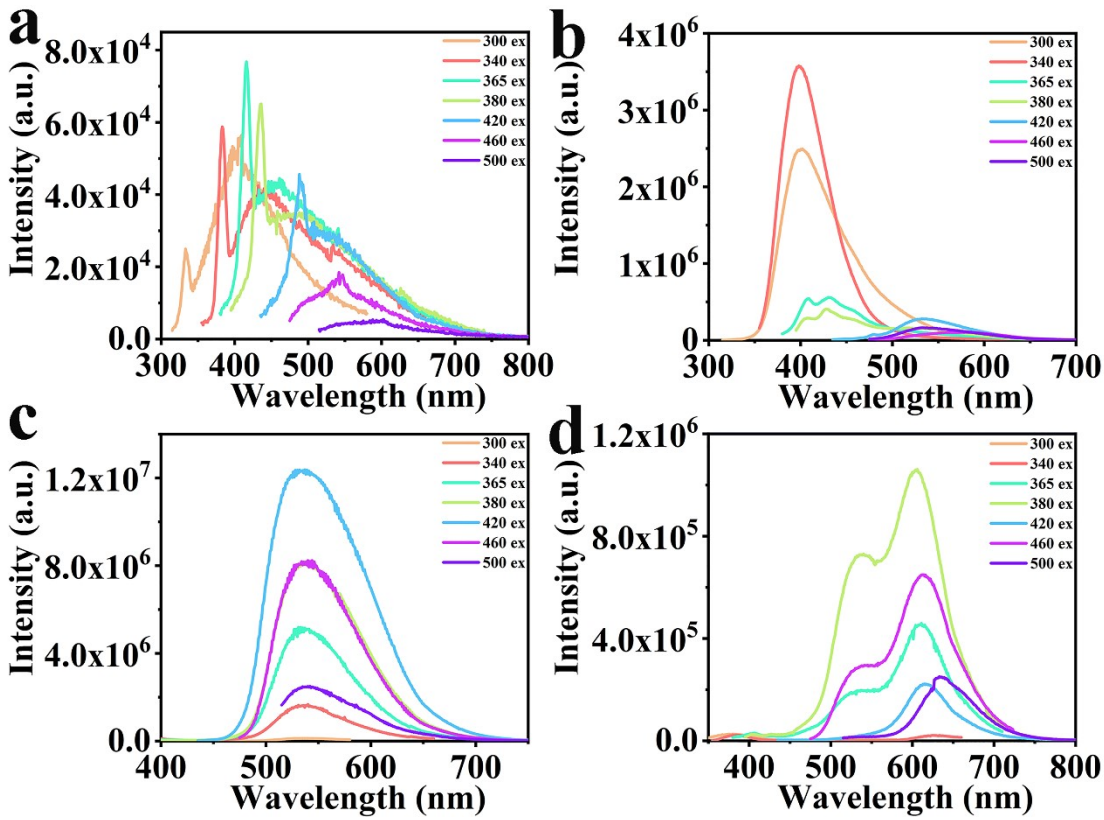

Fig. S11. Emission spectra of (a) OCDs, (b) N,S-BCDs, (c) N,S-GCDs and (d) N, S-RCDs under different excitation wavelengths (300 -500 nm).

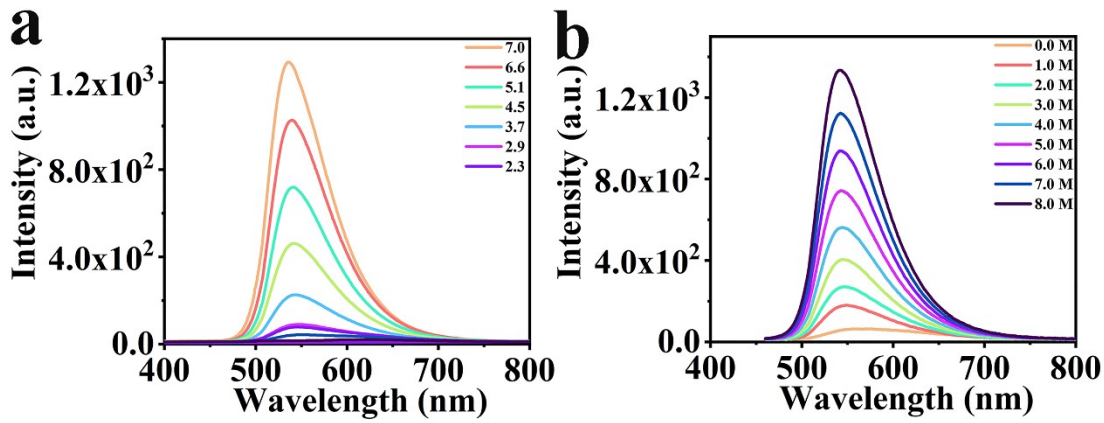

Fig. S12. Emission spectra excited under 435 nm with (a) different pH values (2.3-7.0) and (b) adding different concentrations of alkali (0-8.0 M).

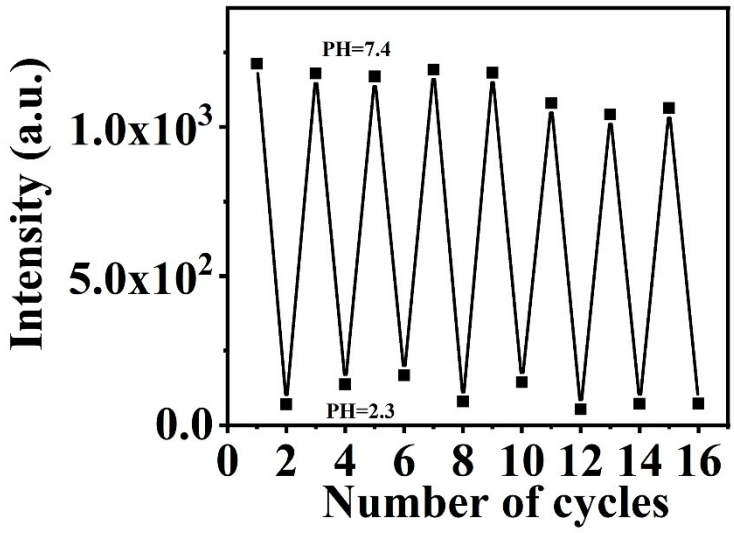

Fig. S13. Fluorescence reversibility against pH value change between 2.3 and 7.4 repeatedly.

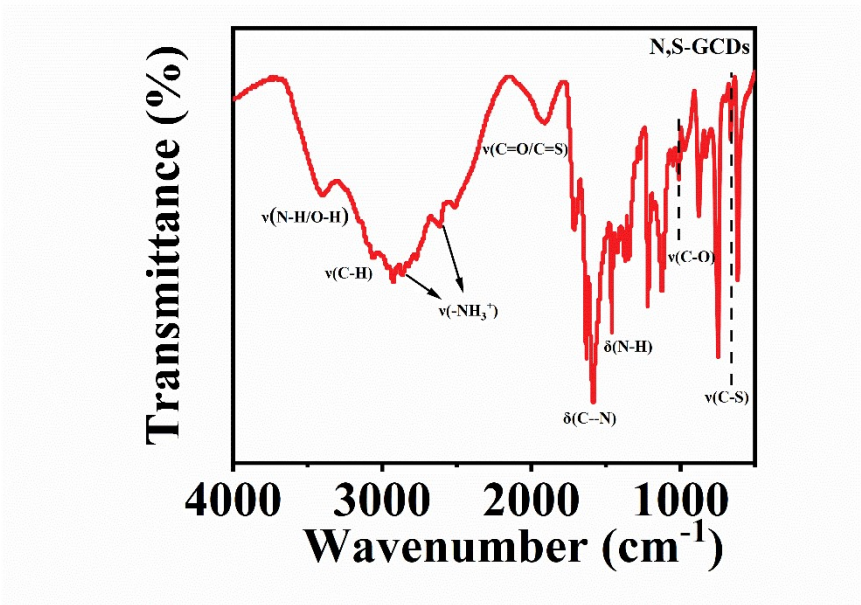

Fig. S14. FT-IR spectra of the prepared N,S-GCDs with adding acid.

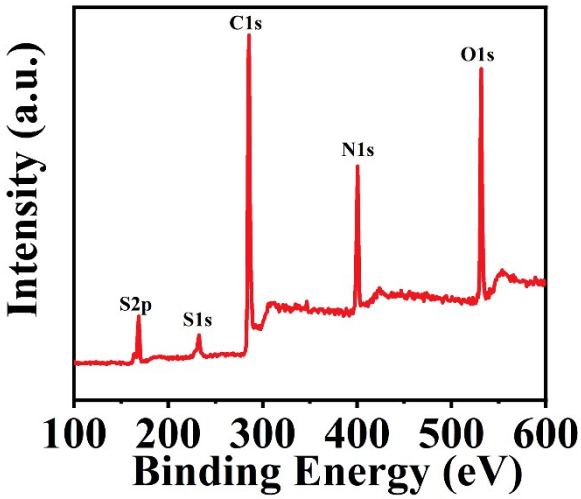

Fig. S15. Full scan XPS spectrum of N,S-GCDs with adding acid.

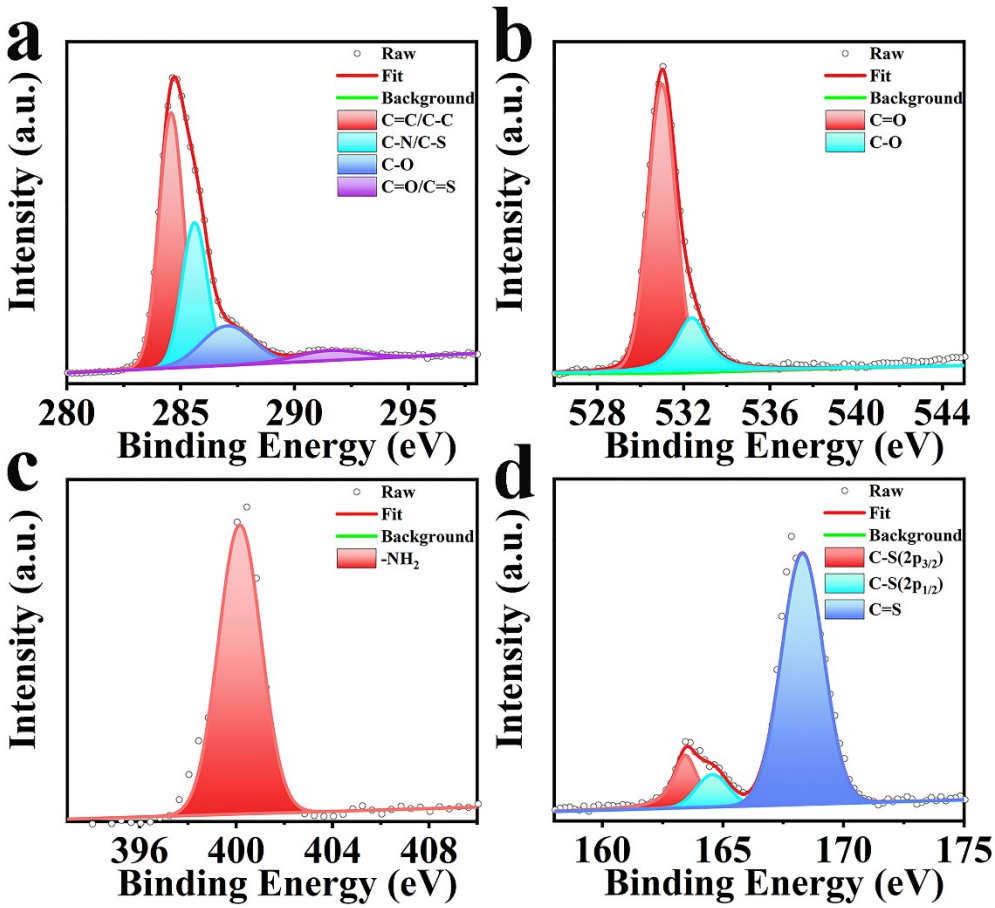

Fig. S16. High resolution XPS spectra of (a) C 1s, (b) O 1s, (c) N 1s and (d) S 2p of the prepared N,S-GCDs with adding acid.

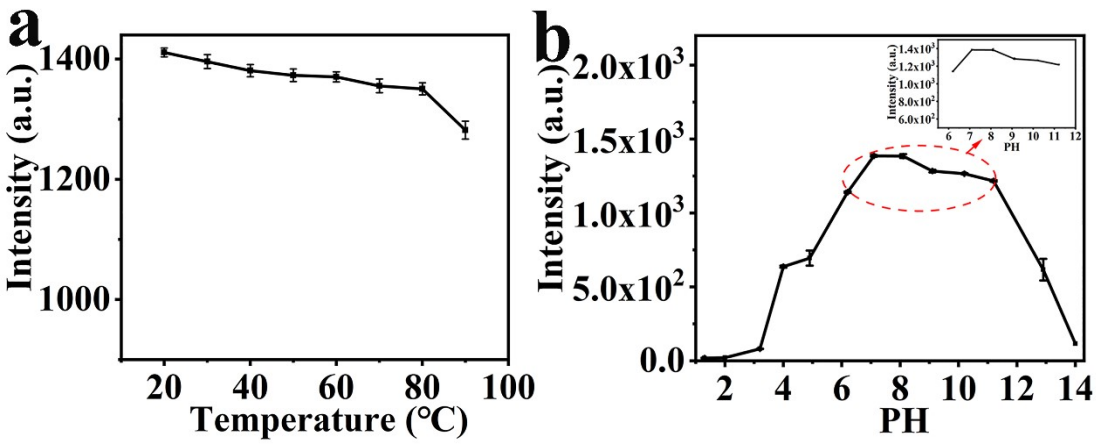

Fig. S17. The effect of (a) different temperatures (20-90 ºC) and (b) various pH values (1-14) on the fluorescence intensities of the N,S-GCDs.

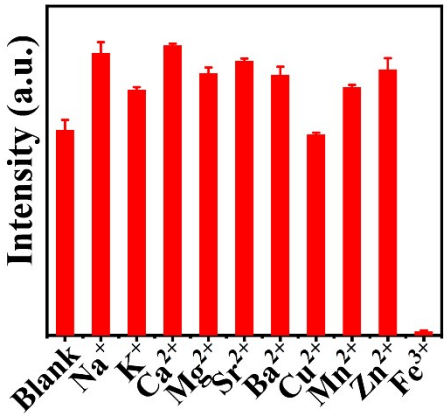

Fig. S18. The effect of different ion solutions (5000 μM) on the fluorescence intensity of the N,S-GCDs.

Table S1. Comparison of QY of CDs synthesized using electrochemical methods.

Precursors	Emission peak (nm)	QY (%)	Refs.
Carbon cloth	~ 450 nm	[c]3.80	[1]
Graphite rods	~510 nm	[c]7.90	[2]
[a]GO powder	~ 450 nm	[c]7.80	[3]
[b]MWCNT	~ 430 nm	[c]6.30	[4]
Carbon fibers	~ 450 nm	[c]1.47	[5]
Graphene oxide nanosheets	~ 455 nm	[c]6.60	[6]
Graphite rods	~ 450 nm	[c]4.0~5.0	[7]
Carbon fibers	~ 500 nm	[c]8.6	[8]
C60 film	~ 430 nm	[c]5.0~6.0	[9]
Graphite rods	~ 541 nm	[d]12.99	**This work**

[a]GO: graphene oxide, [b]MWCNT: multiwalled carbon nanotubes.
c Note: the QY is measured by using quinine sulfate as a reference.
d Note: the QY is absolute quantum yield.

Table S2. Fitted parameters of the fluorescence decay curves of OCDs, N,S-BCDs, N,S-GCDs, and N,S-RCDs.

Sample	**τ_1/(ns) (percent)**	**τ_2/(ns) (percent)**	**τ_{ave} (ns)**	**χ^2**
OCDs	4.88 (76.25 %)	25.82 (23.75 %)	9.85	1.20
N,S-BCDs	5.24 (74.64 %)	0.83 (25.36 %)	4.12	1.05
N,S-GCDs	141.64 (0.74 %)	4.50 (99.26 %)	5.51	1.21
N,S-RCDs	230.38 (2.34 %)	4.21 (97.66%)	9.50	1.06

Table S3. Calculated radiative and non-radiative rate constants of OCDs, N,S-BCDs, N,S-GCDs, and N,S-RCDs. (k_R: radiative rate constants; k_{nR}: non-radiative rate constants).

Sample	**OCDs**	**N,S-BCDs**	**N,S-GCDs**	**N,S-RCDs**
k_R (s^{-1})	4.97×10^7	4.25×10^8	2.36×10^9	1.54×10^8
k_{nR} (s^{-1})	1.01×10^8	2.38×10^8	1.58×10^8	1.04×10^8

Table S4. Fitted parameters of the fluorescence decay curves of N-BCDs, N-GCDs and N-RCDs.

Sample	τ_1/(ns) (percent)	τ_2/(ns) (percent)	τ_{ave}	χ^2
N-BCDs	0.03 (0.02 %)	4.02 (99.98 %)	4.02	1.05
N-GCDs	0.02 (0.01 %)	3.65 (99.99 %)	3.65	1.09
N-RCDs	179.43 (2.72 %)	2.42 (97.28%)	7.23	1.03

Table S5. Calculated radiative and non-radiative rate constants of B CDs-N, N-GCDs and N-RCDs. (k_R: radiative rate constants; k_{nR}: non-radiative rate constants).

Sample	N-BCDs	N-GCDs	N-RCDs
k_R (s^{-1})	2.34×10^8	9.45×10^8	1.09×10^8
k_{nR} (s^{-1})	2.46×10^8	2.65×10^8	1.37×10^8

Table S6. Atomic ratio of characteristic peaks of C1s spectra for OCDs, N,S- BCDs, N,S-GCDs, and N,S-RCDs.

Samples	C=C/C-C (%)	C-N/C-S (%)	C-O (%)	C=O/C=S (%)
OCDs	56.53	-	26.68	16.79
N,S-BCDs	38.15	19.61	17.76	24.48
N,S-GCDs	42.90	31.18	17.77	8.15
N,S-RCDs	48.33	30.01	12.92	8.74

Table S7. Atomic ratio of characteristic peaks of O1s spectra for OCDs, N,S-BCDs, N,S-GCDs, and N,S-RCDs.

Sample	C=O (%)	C-O (%)
OCDs	84.98	15.02
N,S-BCDs	80.69	19.31
N,S-GCDs	82.28	17.72
N,S-RCDs	70.01	29.99

Table S8. Atomic ratio of characteristic peaks of S2p spectra for OCDs, N,S-BCDs, N,S-GCDs, and N,S-RCDs.

Sample	C-S ($2p_{3/2}$) (%)	C-S ($2p_{1/2}$) (%)	C=S (%)
OCDs	-	-	-
N,S-BCDs	13.55	13.59	72.86
N,S-GCDs	14.18	16.72	69.10
N,S-RCDs	10.75	11.72	77.53

Table S9. Relative contents of C, O, N and S elements of the OCDs, N,S-BCDs, N,S-GCDs, and N,S-RCDs on the basis of the XPS spectra.

Samples	C1s (atomic%)	O1s (atomic%)	N1s (atomic%)	S2p (atomic%)
OCDs	66.88	33.12	-	-
N,S-BCDs	64.23	13.73	17.48	4.56
N,S-GCDs	60.90	13.43	20.93	4.74
N,S-RCDs	63.73	12.89	19.51	3.87

Table S10. Relative contents of C, O, and N elements of the N-BCDs, N-GCDs and N-RCDs on the basis of the XPS spectra.

Sample	C1s (atomic %)	O1s (atomic %)	N1s (atomic %)
N-BCDs	74.18	15.02	10.80
N-GCDs	71.80	14.32	13.88
N-RCDs	74.64	6.21	19.15

Table S11. Atomic ratio of characteristic peaks of C1s spectra for N-BCDs, N-GCDs and N-RCDs.

Samples	C=C/C-C (%)	C-N (%)	C-O (%)	C=O (%)
N-BCDs	32.45	41.01	21.60	4.94
N-GCDs	28.09	51.59	12.74	7.58
N-RCDs	26.01	54.10	9.55	10.34

Table S12. Atomic ratio of characteristic peaks of XPS O1s spectra for N-BCDs, N-GCDs and N-RCDs.

Samples	C=O (%)	C-O (%)
N-BCDs	57.46	42.54
N-GCDs	68.60	31.40
N-RCDs	74.22	25.78

Table S13. Relative contents of C, O, N and S elements of N,S-GCDs with adding acid on the basis of the XPS data.

Sample	C1s (atomic%)	O1s (atomic%)	N1s (atomic%)	S2p (atomic%)
N,S-GCDs	62.32	15.82	17.44	4.42

Table S14. Atomic ratio of characteristic peaks of XPS C1s, O1s and S2p spectra for N,S-GCDs with adding acid.

Sample	C1s				O1s		S2p		
	C=C/C-C (%)	C-N/C-S (%)	C-O (%)	C=O/C=S (%)	C=O (%)	C-O (%)	C-S ($2p_{3/2}$) (%)	C-S ($2p_{1/2}$) (%)	C=S (%)
N,S-GCDs	50.15	28.79	15.97	5.09	77.37	22.63	13.29	7.80	78.91

References:

[1] J. L. Chang, C. W. Liao, D. Arthisree, A. S. Kumar, J. M. Zen, A size-controlled graphene oxide materials obtained by one-step electrochemical exfoliation of carbon fiber cloth for applications to in situ gold nanoparticle formation and electrochemical sensors-a preliminary study, Biosensors 12 (2022) 360.

[2] X. C. Fu, J. Z. Jin, J. Wu, J. C. Jin, C. G. Xie, A novel turn-on fluorescent sensor

for highly selective detection of Al(III) in an aqueous solution based on simple electrochemically synthesized carbon dots, Anal. Methods 9 (2017) 3941-3948.

[3] J. Deng, Q. Lu, H. Li, Y. Zhang, S. Yao, Large scale preparation of graphene quantum dots from graphite oxide in pure water via one-step electrochemical tailoring, RSC Adv. 5 (2015) 29704-29707

[4] D. B. Shinde, V. K. Pillai, Electrochemical preparation of luminescent graphene quantum dots from multiwalled carbon nanotubes, Chem. Eur. J. 18 (2012) 12522-12528.

[5] L. Bao, Z. L. Zhang, Z. Q. Tian, L. Zhang, C. Liu, Y. Lin, B. Qi, D. W. Pang, Electrochemical tuning of luminescent carbon nanodots: from preparation to luminescence mechanism, Adv. Mater. 23 (2011) 5801-5806.

[6] R. Qiang, W. Sun, K. Hou, Z. Li, J. Zhang, Y. Ding, J. Wang, S. Yang, Electrochemical trimming of graphene oxide affords graphene quantum dots for Fe^{3+} detection, ACS Appl. Nano Mater. 4 (2021) 5220-5229.

[7] K. Chu, J. R. Adsetts, S. He, Z. Zhan, L. Yang, J. M. Wong, D. A. Love, Z. Ding, Electrogenerated chemiluminescence and electroluminescence of N-doped graphene quantum dots fabricated from an electrochemical exfoliation process in nitrogen-containing electrolytes, Chem. Eur. J. 26 (2020) 15892-15900.

[8] Y. Yan, H. Li, Q. Wang, H. Mao, W. Kun, Controllable ionic liquid-assisted electrochemical exfoliation of carbon fibers for the green and large-scale preparation of functionalized graphene quantum dots endowed with multicolor emission and size, J. Mater. Chem. C 5 (2017) 6092-6100.

[9] Y. E, L. Bai, L. Fan, M. Han, X. Zhang, S. Yang, Electrochemically generated fluorescent fullerene 60 nanoparticles as a new and viable bioimaging platform, J. Mater. Chem. 21 (2011) 819-823.